0026-895X/92/020307-04$03.00/0

MOLECULAR PHARMACOLOGY, 42:307-310

Evidence for the Stereoselective Inhibition of Chick Embryo Hepatic Ferrochelatase by *N*-Alkylated Porphyrins. II

S. M. KIMMETT, R. A. WHITNEY, and G. S. MARKS

Departments of Pharmacology and Toxicology (S.M.K., G.S.M.) and Chemistry (R.A.W.), Queen's University, Kingston, Ontario, Canada K7L 3N6

Received February 5, 1992; Accepted May 4, 1992

SUMMARY

N-Ethylprotoporphyrin (*N*-ethyl-PP) was isolated from the livers of phenobarbital-pretreated rats after the administration of 3,5-diethoxycarbonyl-1,4-dihydro-2,6-dimethyl-4-ethylpyridine, separated into its four regioisomers by high performance liquid chromatography, and quantitated. The percentage ratio, in the chromatogram, of the peak areas of the ring A-substituted (N_A) and the ring B-substituted (N_B) regioisomers was 80:20, compared with 50:50 for synthetic *N*-ethyl-PP. The N_A regioisomer of *N*-ethyl-PP isolated from rat liver was found to be approximately 5 times more potent an inhibitor of ferrochelatase than was the N_B regioisomer. Because the synthetic N_A regioisomer (an equal mixture of the N_A and the epi-N_A enantiomers) is equipotent with the synthetic N_B regioisomer (an equal mixture of the N_B and the epi-N_B enantiomers), epi-N_B must be more potent than epi-N_A. The higher potency previously observed with the N_A plus N_B regioisomers of *N*-ethyl-PP isolated from rat liver, compared with the N_A plus N_B regioisomers of synthetic *N*-ethyl-PP, is explained by the fact that the biological preparation contains 80% of the potent N_A, compared with 25% of the potent N_A and 25% of the potent epi-N_B in the synthetic preparation. The critical features for optimal ferrochelatase-inhibitory activity are the ring A *N*-ethyl group facing downward in the N_A isomer and the ring B *N*-ethyl group in the epi-N_B isomer being rotated through 180° to occupy the same position. According to one proposed mechanism, *N*-alkylprotoporphyrins inhibit ferrochelatase by serving as transition state analogues for the iron insertion step. X-ray crystallography shows that the *N*-alkyl group-bearing pyrrole ring and the pyrrole ring opposite to the *N*-alkyl group are tilted out of planarity in opposite directions. We suggest that this tilting reflects the normal conformational changes required for the insertion of iron into the protoporphyrin IX ring by ferrochelatase and that the greater inhibitory activity of N_A and epi-N_B isomers, compared with epi-N_A and N_B isomers, is due to the fact that the normal mechanism for ferrochelatase-catalyzed iron insertion has preference for an A-C ring tilt over a B-D ring tilt.

The porphyrinogenic agent 4-ethyl-DDC (Fig. 1), when administered to rodents, results in mechanism-based inactivation of hepatic microsomal cytochrome P450 and hepatic accumulation of the four regioisomers of *N*-ethyl-PP (1, 2). The N_A and N_B regioisomers (Fig. 2) of *N*-ethyl-PP, but not the N_C and N_D regioisomers, are potent inhibitors of ferrochelatase (EC 4.99.1.1) activity (2).[1]

In the chemical synthesis of *N*-ethyl-PP, alkylation occurs from both sides of the protoporphyrin IX ring, giving an optically inactive racemic mixture of regioisomers. In contrast, the orientation of the heme moiety within the active site of cytochrome P450 is such that alkylation can occur from only one side of the protoporphyrin IX ring, resulting in the formation of an optically active *N*-alkyl-PP (3). From the studies of Ortiz de Montellano *et al.* (3), it can be deduced that the A and B ring regioisomers of *N*-ethyl-PP, obtained from rat liver, have the configuration shown in Fig. 2, with the *N*-ethyl group facing downward (N_A regioisomer, Fig. 2a; N_B regioisomer, Fig. 2c).[2] The synthetic mixture of A- and B-ring regioisomers, therefore, consists of two pairs of enantiomers, *viz.*, N_A-ethyl-PP (Fig. 2a) and epi-N_A-ethyl-PP (Fig. 2b) and N_B-ethyl-PP (Fig. 2c) and epi-N_B-ethyl-PP (Fig. 2d). We have shown that the combined ring A and B regioisomers of *N*-ethyl-PP, isolated from rat liver, are more potent inhibitors of ferrochelatase than are the combined ring A and B regioisomers of synthetic *N*-ethyl-PP (4). We have also shown that the synthetic N_A regioisomer of *N*-ethyl-PP (an equal mixture of the N_A and epi-N_A enantiomers) is equipotent with the synthetic N_B regioisomer (an equal mixture of the N_B and epi-N_B enantiomers) (2). We have

This work was supported by the Medical Research Council of Canada.

[1] N_A and epi-N_A refer to the two enantiomers of the ring A-substituted regioisomer of an *N*-alkyl-PP (biological N_A is a single enantiomer, and synthetic N_A is a racemic mixture of N_A and epi-N_A); N_B and epi-N_B refer to the two enantiomers of the ring B-substituted regioisomer of an *N*-alkyl-PP (biological N_B is a single enantiomer, and synthetic N_B is a racemic mixture of N_B and epi-N_B). The same applies for the N_C and N_D regioisomers.

[2] To define the orientation of the *N*-alkyl group relative to the plane of the porphyrin ring, the following convention is used: if the pyrrole rings A, B, C, and D are in a clockwise arrangement in the plane of the paper, then "downward" indicates that the *N*-alkyl group lies below the plane of the paper and "upward" indicates that the *N*-alkyl group lies above the plane of the paper.

ABBREVIATIONS: 4-ethyl-DDC, 3,5-diethoxycarbonyl-1,4-dihydro-2,6-dimethyl-4-ethylpyridine; TLC, thin layer chromatography; HPLC, high performance liquid chromatography; *N*-ethyl-PP, *N*-ethylprotoporphyrin; *N*-alkyl-PP, *N*-alkylprotoporphyrin.

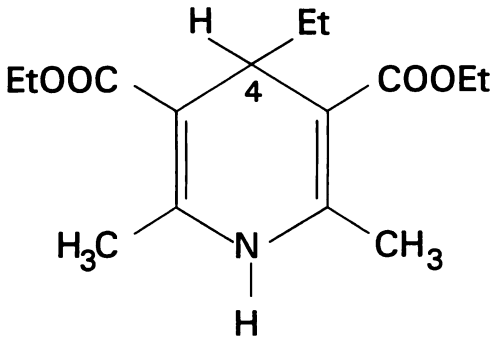

Fig. 1. Structure of 4-ethyl-DDC. *Et*, ethyl.

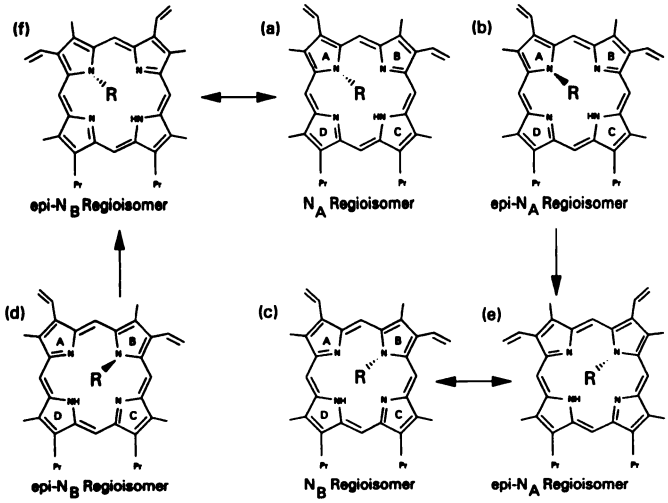

Fig. 2. Configuration of the N_A and N_B regioisomers and enantiomers of *N*-ethyl-PP (*R*, ethyl).

previously made the assumption that the N_A and N_B regioisomers are equipotent as ferrochelatase inhibitors (4). It follows, therefore, that the N_A regioisomer (Fig. 2a) is more potent than the epi-N_A regioisomer (Fig. 2b) and that the N_B regioisomer is more potent than the epi-N_B regioisomer (Fig. 2d) (4). In view of this difference in potency, it was thought likely that the regioisomers would bind to the active site of ferrochelatase with the *N*-alkyl group facing downward (Fig. 2, a and c).

By rotation, the epi-N_A regioisomer (Fig. 2e) is an "analogue" of the N_B regioisomer (Fig. 2c), with a different orientation of the vinyl and methyl groups on rings A and B. In a similar way, the epi-N_B regioisomer (Fig. 2f) is an "analogue" of the N_A regioisomer (Fig. 2a). The higher potency of the N_A and N_B regioisomers, compared with their corresponding enantiomers (epi-N_A and epi-N_B), suggests that the ferrochelatase active site must be discriminating between the enantiomers N_A and epi-N_A, and N_B and epi-N_B, by virtue of the position of the methyl and vinyl groups. It was concluded that the interaction of the methyl and vinyl substituents with the active site of ferrochelatase should be considered a hydrophobic interaction, with specific requirements for the positioning of the methyl and vinyl substituents (4).

The weakness of the argument described above was the assumption that the N_A and N_B regioisomers (Fig. 2, a and c, respectively) are equiactive. Our objective in the present study was to isolate the individual N_A and N_B regioisomers from *N*-ethyl-PP obtained from rat liver and to compare their potency as ferrochelatase inhibitors. The synthetic N_A and N_B regioisomers, as racemates, had previously been found to be equipotent as ferrochelatase inhibitors (2).

Materials and Methods

Reagents and chemicals. Protoporphyrin IX and mesoporphyrin IX were obtained from Porphyrin Products (Logan, UT). Tetrahydrofuran (stabilized with 250 ppm butylated hydroxytoluene), hexane, methanol, acetone, and dichloromethane were HPLC grade and were purchased from British Drug Houses Inc. (Toronto, Ontario, Canada). Waymouth MD 705/1 medium was purchased from GIBCO (Grand Island, NY).

Preparation and purification of *N*-ethyl-PP. *N*-Ethyl-PP was synthesized by reacting protoporphyrin IX (3.2 mg) with ethyl iodide (2.0 ml) for 18 hr at 108° (5). Biological *N*-ethyl-PP was isolated from the livers of phenobarbital-pretreated rats after the administration of 4-ethyl-DDC (1, 4). The zinc-complexed *N*-ethyl-PP dimethyl esters were separated into the N_A and/or N_B regioisomers and the N_C and/or N_D regioisomers by two consecutive TLC procedures.[3] The first TLC purification of the Zn-*N*-ethyl-PP was on Analtech (2000-μm) silica gel G plates (20 × 20 cm), developed in dichloromethane/methanol (20:3). A single green band (R_F, 0.55–0.62) that fluoresced red under UV light was eluted from the plate with acetone and evaporated to dryness. The residue was redissolved in dichloromethane, applied to Analtech (1000-μm) silica gel G plates, and developed in dichloromethane/acetone (5:1). Two green bands (R_F, 0.69–0.72 and 0.74–0.77)[3] that fluoresced red under UV light were eluted separately from the plates with acetone and evaporated to dryness. Dichloromethane was added, and the electronic absorption spectra were determined using a Hewlett Packard 8451A diode array spectrophotometer (6). The concentration of the zinc-complexed *N*-ethyl-PPs was determined by using the molar extinction coefficient for Zn-*N*-methylprotoporphyrin (124,000 M^{-1} cm^{-1} at 432 nm) (7).

Purification and separation of the regioisomers of *N*-ethyl-PP. The Zn-*N*-ethyl-PPs, consisting of the N_A and/or N_B regioisomers or the N_C and/or N_D regioisomers, were individually purified by HPLC (7) on a Whatman Partisil 10 PAC column (4.6 × 250 mm), eluted with a 20-min linear gradient (0–100%) of methanol in hexane/tetrahydrofuran (1:1), at a flow rate of 1.0 ml/min. Absorption was monitored at 432 nm, using a variable-wavelength detector. Fractions with the characteristic spectrum of Zn-*N*-ethyl-PP were pooled, and the zinc cation was removed by treatment with 5% sulfuric acid/methanol (8). The zinc-free *N*-ethyl-PPs were separated into N_A and N_B regioisomers or N_C and N_D regioisomers by using a second Partisil 10 PAC column.[3] The regioisomers were eluted isocratically with hexane/tetrahydrofuran/methanol/water (49.2:49.2:1.5:0.1), at a flow rate of 0.5 ml/min. Absorption was monitored at 420 nm. The peaks were collected separately, and their electronic absorption spectra were compared with those previously observed (1, 9).

Ferrochelatase-inhibitory activity. The N_A and N_B regioisomers of *N*-ethyl-PP dimethyl ester were converted to free acids by hydrolysis in 300 μl of 6.0 N hydrochloric acid overnight, in the dark, at room temperature (8). After removal of the hydrochloric acid under a stream of nitrogen, the *N*-ethyl-PPs were dissolved in 95% ethanol, and a series of dilutions were prepared. Aliquots (0.1 ml in 95% ethanol) were transferred to the sidearm of Thunberg tubes. Control tubes received 0.1 ml of 95% ethanol.

Details of the cell culture technique have previously been reported (10, 11). The 18-day-old chick embryo liver cells were maintained in 10-cm-diameter plastic Petri dishes containing 15 ml of serum-free Waymouth MD 705/1 medium supplemented with penicillin G sodium (60 mg/L), streptomycin sulfate (100mg/L), sodium bicarbonate (2.24 g/L), insulin (1 mg/L), and L-thyroxine sodium pentahydrate (1mg/L).

[3] S. M. Kimmett, and G. S. Marks. Thin layer chromatographic separation of the ferrochelatase-inhibitory ring A and ring B regioisomers of *N*-ethylprotoporphyrin from a mixture of the four regioisomers. Submitted for publication.

After a 24-hr incubation at 37°, the medium was replaced. After an additional 24-hr incubation, the cells were harvested with a buffer containing 0.25 M sucrose, 0.05 M Tris·HCl, and 1.0 mM EDTA, at pH 8.2. The cells were centrifuged for 5 min at 500 × *g*, washed with the sucrose-Tris buffer (1.0 ml/Petri dish), and homogenized in 0.6 ml/dish 0.02 M Tris·HCl buffer (pH 8.2). Aliquots (0.9 ml) were transferred to the sidearm of the Thunberg tubes containing the *N*-ethyl-PP (0.1 ml).

The body of the Thunberg tubes contained mesoporphyrin IX (120 nmol), 1% (w/v) Tween 80 (0.3 ml), 95% ethanol (0.3 ml), 0.2 M Tris·HCl buffer, pH 8.2 (1.5 ml), 0.2 M dithioerythritol (60 μl), and 1.0 mM ferrous sulfate (120 μl). The sidearm was connected to the body of the Thunberg tube, and the atmosphere was made anaerobic by alternating vacuum with nitrogen, several times. After a 5-min preincubation in a 37° water bath, the contents of the sidearm were tipped into the body of the Thunberg tubes for a 10-min incubation at 37°. The reaction was terminated by the addition of 0.4 M iodoacetamide (0.5 ml) to the tubes.

The amount of mesoheme formed was determined by using the reduced versus oxidized spectrum of the pyridine mesohemochromogen (6, 10, 12), recorded from 500 to 560 nm on a Hewlett Packard 8451A diode array spectrophotometer. Ferrochelatase activity was expressed as nmol of mesoheme formed/mg of protein/10 min. Protein was measured by the method of Lowry *et al.* (13).

Results and Discussion

TLC purification of *N*-ethyl-PP. The two fluorescing green bands produced by the TLC purification of Zn-*N*-ethyl-PP have previously been identified as the N_A and/or N_B regioisomers, in the band further from the origin (R_F, 0.74–0.77), and the N_C and/or N_D regioisomers, in the lower band (R_f, 0.69–0.72).[3] The electronic absorption spectrum of the zinc-complexed N_A and/or N_B regioisomers has a shoulder on the Soret band at 432 nm (1, 7). This shoulder is not present in the spectrum of the zinc-complexed N_C and/or N_D regioisomers (1, 7). The electronic absorption spectra were used to quantitate the regioisomer composition of Zn-*N*-ethyl-PP in each TLC band. The N_A and/or N_B regioisomers comprised 36% of the total regioisomers (N_A plus N_B plus N_C plus N_D) for synthetic Zn-*N*-ethyl-PP and 68% of the total regioisomers for biological Zn-*N*-ethyl-PP. These results are similar to those previously found in this laboratory (4).

HPLC separation of the regioisomers of *N*-ethyl-PP. Two consecutive HPLC procedures, as previously described,[3] were used to obtain the individual regioisomers of *N*-ethyl-PP. The order of regioisomer elution previously observed was N_B, N_A and N_C, N_D regioisomers (1). We found that 0.1% water was needed in the isocratic solvent system to obtain separation of the regioisomers. Other investigators reported separation of the regioisomers without the addition of water to their solvent systems (1, 7).

A sample of the N_A plus N_B regioisomers obtained from rat liver was injected onto the HPLC column, and the peak area of the N_B regioisomer was significantly less than the peak area of the N_A regioisomer, i.e., the percentage ratio of N_A:N_B was 80:20. However, when a sample of synthetic *N*-ethyl-PP containing the N_A (N_A plus epi-N_A) plus N_B (N_B plus epi-N_B) regioisomers was injected onto the HPLC column, two peaks of equal area were eluted, i.e., the percentage ratio of N_A:N_B was 50:50.

Ferrochelatase-inhibitory activity. The data in Fig. 3a show that the synthetic N_A and N_B regioisomers of *N*-ethyl-PP are equally potent as inhibitors of chick embryo liver ferrochelatase activity, confirming previous results obtained with a rat liver ferrochelatase preparation (2). However, a comparison of the N_A and N_B regioisomers of biological *N*-ethyl-PP showed that the N_A regioisomer is approximately 5 times more potent an inhibitor of ferrochelatase than is the biological N_B regioisomer (Fig. 3b). This result shows clearly that the previous assumption that the N_A regioisomer (Fig. 2a) is equipotent with the N_B regioisomer (Fig. 2c) (4) is incorrect. Moreover, the conclusions derived from the previous assumption, *viz.*, that the ferrochelatase active site must be discriminating among the pairs of enantiomers (N_A versus epi-N_A and N_B versus epi-N_B) by virtue of the difference in position of the methyl and vinyl groups on rings A and B (4), must also be incorrect. We now know that the N_A regioisomer has 5 times the potency of the N_B regioisomer (eq. 1) and the synthetic N_A regioisomer (N_A plus epi-N_A) is equipotent with the synthetic N_B regioisomer (N_B plus epi-N_B) (eq. 2).

$$N_A = 5N_B \quad (1)$$

$$N_A + \text{epi-}N_A = N_B + \text{epi-}N_B \quad (2)$$

Substituting $5N_B$ for N_A in eq. 2,

$$5N_B + \text{epi-}N_A = N_B + \text{epi-}N_B$$

Therefore,

$$4N_B + \text{epi-}N_A = \text{epi-}N_B \quad (3)$$

From eq. 3, we are able to conclude that epi-N_B is more potent than epi-N_A and epi-N_B is more potent than N_B, because it would take four N_B plus one epi-N_A to equal one epi-N_B.

It may be concluded that the ferrochelatase active site does not discriminate among the regioisomers and enantiomers by virtue of the difference in the position of methyl and vinyl groups. What does emerge as being critical for optimal activity is the ring A *N*-ethyl group facing downward in the N_A regioisomer (Fig. 2a) and the ring B *N*-ethyl group in the epi-N_B regioisomer (Fig. 2d) being rotated through 180° to occupy the same position (Fig. 2f). It can be concluded that none of the positions assumed, or capable of being assumed, by the *N*-ethyl

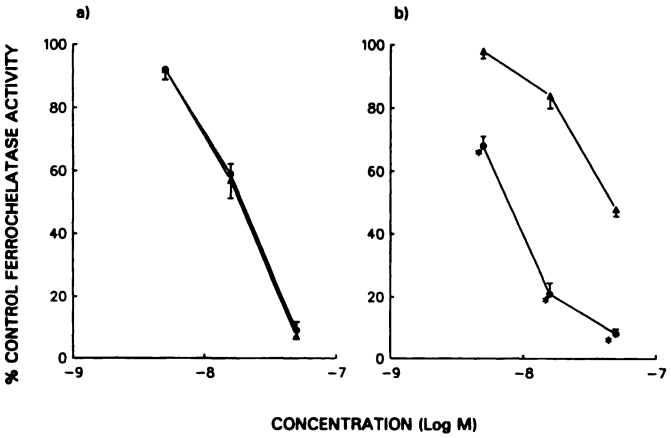

Fig. 3. Percentage of control ferrochelatase activity of chick embryo liver cell cultures after incubation with the N_A regioisomer (●) or the N_B regioisomer (▲) of synthetic *N*-ethyl-PP (a) or biological *N*-ethyl-PP (b). Each *point* represents the mean ± standard deviation of three to five determinations in one experiment; the results were confirmed in two additional experiments. *, Significantly different from the same concentration of the N_B regioisomer of *N*-ethyl-PP, as determined by Student's unpaired *t* test ($p < 0.05$).

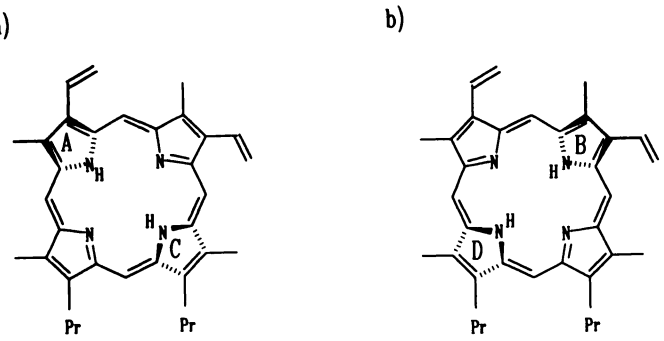

Fig. 4. Structure of protoporphyrin IX, showing the conformational changes associated with the iron insertion step. a, Rings A and C tilted in opposite directions; b, rings B and D tilted in opposite directions. Pr, propionic acid).

group of the N_B regioisomer (Fig. 2c) or the epi-N_A regioisomer (Fig. 2, b and e) provides for optimal activity.

If the orientations of *N*-ethyl-PPs depicted in Fig. 2, a and f, represent the optimal structure for ferrochelatase inhibition, whereas those depicted in Fig. 2, c and e, are less than optimal, then the origin of this difference in inhibitory activity must be addressed. The proposed enzyme mechanism for ferrochelatase (14) involves four sequential steps. These are (i) binding of ferrous iron, (ii) binding of protoporphyrin IX, (iii) insertion of iron into the porphyrin macrocycle, and (iv) release of heme from the enzyme. Furthermore, according to this mechanism (14), the role of *N*-alkyl-PPs in inhibiting ferrochelatase is a consequence of their ability to serve as transition state analogues for the iron insertion step. X-ray crystallographic structures of *N*-alkyl-PP derivatives have shown (15) that the *N*-alkyl group-bearing pyrrole ring and the pyrrole ring opposite to the *N*-alkyl group (i.e., rings A and C or B and D) are tilted out of planarity in opposite directions. Presumably, this tilting in the transition state analogues reflects the normal conformational changes required for the insertion of iron into protoporphyrin IX, as catalyzed by ferrochelatase. If this is the case, then the greater inhibitory activity of N_A and epi-N_B isomers (as depicted in Fig. 2, a and f), compared with epi-N_A and N_B isomers (as depicted in Fig. 2, c and e), suggests that the normal mechanism for ferrochelatase-catalyzed iron insertion has preference for an A-C ring tilt (Fig. 4a) over a B-D ring tilt (Fig. 4b).

Finally, how do we explain the fact that the N_A and N_B regioisomer mixture derived from rat liver was more potent than the mixture of the N_A and N_B regioisomers derived from a synthetic route? It will be recalled that HPLC separation demonstrated that the percentage ratio of the peak areas of the N_A and N_B regioisomers was 50:50 in synthetic *N*-ethyl-PP (eq. 4) and that the percentage ratio of the N_A and N_B regioisomers in biological *N*-ethyl-PP was 80:20 (eq. 5). The composition of synthetic *N*-ethyl-PP is

$$25\%\ N_A + 25\%\ \text{epi-}N_A + 25\%\ N_B + 25\%\ \text{epi-}N_B \quad (4)$$

and the composition of biological *N*-ethyl-PP is

$$80\%\ N_A + 20\%\ N_B \quad (5)$$

Because N_A is 5 times more potent than N_B and epi-N_B is more potent than epi-N_A, the higher potency of the biological *N*-ethyl-PP, compared with the synthetic *N*-ethyl-PP, is explained by the fact that the biological preparation contains 80% of the potent N_A, compared with 25% of the potent N_A and 25% of the potent epi-N_B in the synthetic preparation.

References

1. Ortiz de Montellano, P. R., H. S. Beilan, and K. L. Kunze. *N*-Alkylprotoporphyrin IX formation in 3,5-dicarbethoxy-1,4-dihydrocollidine-treated rats: transfer of the alkyl group from the substrate to the porphyrin. *J. Biol. Chem.* **256**:6708–6713 (1981).
2. Ortiz de Montellano, P. R., K. L. Kunze, S. P. C. Cole, and G. S. Marks. Differential inhibition of hepatic ferrochelatase by the isomers of *N*-ethylprotoporphyrin IX. *Biochem. Biophys. Res. Commun.* **103**:581–586 (1981).
3. Ortiz de Montellano, P. R., K. L. Kunze, and H. S. Beilan. Chiral orientation of prosthetic heme in the cytochrome P-450 active site. *J. Biol. Chem.* **258**:45–47 (1983).
4. McCluskey, S. A., R. A. Whitney, and G. S. Marks. Evidence for the stereoselective inhibition of chick embryo hepatic ferrochelatase by *N*-alkylated porphyrins. *Mol. Pharmacol.* **36**:608–614 (1989).
5. De Matteis, F., A. H. Gibbs, and A. G. Smith. Inhibition of protohaem ferrolyase by *N*-substituted porphyrins: structural requirements for the inhibitory effect. *Biochem. J.* **189**:645–648 (1980).
6. McCluskey, S. A., G. S. Marks, R. A. Whitney, and P. R. Ortiz de Montellano. Differential inhibition of hepatic ferrochelatase by regioisomers of *N*-butyl-, *N*-pentyl-, *N*-hexyl-, and *N*-isobutylprotoporphyrin IX. *Mol. Pharmacol.* **34**:80–86 (1988).
7. Ortiz de Montellano, P. R., H. S. Beilan, and K. L. Kunze. *N*-Methylprotoporphyrin IX: chemical synthesis and identification as the green pigment produced by 3,5-diethoxycarbonyl-1,4-dihydrocollidine treatment. *Proc. Natl. Acad. Sci. USA* **78**:1490–1494 (1981).
8. Ortiz de Montellano, P. R., G. S. Yost, B. A. Mico, S. E. Dinizo, M. A. Correia, and H. Kumbara. Destruction of cytochrome P-450 by 2-isopropyl-4-pentenamide and methyl 2-isopropyl-4-pentenoate: mass spectrometric characterization of the prosthetic heme adducts and nonparticipation of epoxide metabolites. *Arch. Biochem. Biophys.* **197**:524–533 (1979).
9. De Matteis, F., A. H. Gibbs, P. B. Farmer, and J. H. Lamb. Liver production of *N*-alkylated porphyrins caused in mice by treatment with substituted dihydropyridines: evidence that the alkyl group on the pyrrole nitrogen atom originates from the drug. *FEBS Lett.* **129**:328–331 (1981).
10. Cole, S. P. C., E. J. Vavasour, and G. S. Marks. Drug-induced porphyrin biosynthesis. XIX. Potentiation of the porphyrin-inducing effects of SKF 525-A in the chick embryo liver by 3,5-diethoxycarbonyl-1,4-dihydro-2,4,6-trimethylpyridine, an inhibitor of ferrochelatase. *Biochem. Pharmacol.* **28**:3533–3538 (1979).
11. Morgan, R. O., P. W. F. Fisher, J. K. Stephens, and G. S. Marks. Thyroid hormone enhancement of drug-induced porphyrin biosynthesis in chick embryo liver cells maintained in serum-free Waymouth medium. *Biochem. Pharmacol.* **25**:2609–2612 (1976).
12. Porra, R. J., and O. T. G. Jones. Studies on ferrochelatase. I. Assay and properties of ferrochelatase from a pig-liver mitochondrial extract. *Biochem. J.* **87**:181–185 (1963).
13. Lowry, O. H., N. J. Rosebrough, A. L. Farr, and R. J. Randall. Protein measurement with the Folin phenol reagent. *J. Biol. Chem.* **193**:265–275 (1951).
14. Dailey, H. A. *Biosynthesis of Heme and Chlorophylls*. McGraw-Hill, New York, 133–149 (1990).
15. Scheidt, W. R., and Y. J. Lee. *Structure and Bonding*, Vol. 64. Springer-Verlag, Berlin, 1–70 (1987).

Send reprint requests to: Dr. Gerald S. Marks, Department of Pharmacology and Toxicology, Botterell Hall, Queen's University, Kingston, Ontario, K7L 3N6 Canada.